


## Extracting the Quantum Hall Conductance from a Single Bulk Wave Function

Ruihua Fan, Rahul Sahay<sup>✉</sup>, and Ashvin Vishwanath

*Department of Physics, Harvard University, Cambridge, Massachusetts 02138, USA*

 (Received 30 August 2022; revised 30 August 2023; accepted 6 September 2023; published 1 November 2023)

We propose a new formula that extracts the quantum Hall conductance from a single  $(2 + 1)D$  gapped wave function. The formula applies to general many-body systems that conserve particle number, and is based on the concept of modular flow, i.e., unitary dynamics generated from the entanglement structure of the wave function. The formula is shown to satisfy all formal properties of the Hall conductance: it is odd under time reversal and reflection, even under charge conjugation, universal and topologically rigid in the thermodynamic limit. Further evidence for relating the formula to the Hall conductance is obtained from conformal field theory arguments. Finally, we numerically check the formula by applying it to a noninteracting Chern band where excellent agreement is obtained.

DOI: [10.1103/PhysRevLett.131.186301](https://doi.org/10.1103/PhysRevLett.131.186301)

Since the discovery of the quantum Hall effect, the investigation of gapped topological phases has been at the forefront of quantum many-body physics [1–3]. Such phases cannot be characterized by any local order parameters and all of their unusual properties emerge from the entanglement of the ground state wave function [4]. Quantifying this connection has been a persistent and interesting challenge for the past few decades.

For example, entanglement entropy in a ground state wave function reveals the total quantum dimension of anyons [5–7] while access to multiple ground states on a torus allows for a determination of modular matrices characterizing the anyons [8,9]. Further information, such as the entanglement spectrum, reveals the protected edge states [6,7,10–16]. Yet, how to extract the quantum Hall conductance, the first discovered topological quantity, from the entanglement pattern of a gapped wave function alone remains an open question. Here, by gapped wave function, we mean the ground state wave function of a gapped, local Hamiltonian. Solving this question also provides an entanglement characterization of the boundary chiral anomaly via the bulk-edge correspondence. Besides its foundational interest, evaluating such a formula in various variational ansatz of wave functions could help characterize limits to the efficient representations of quantum states especially by tensor networks or stabilizers [17–21].

There are several approaches to extracting Hall conductance that do not invoke entanglement. For free fermion systems, there are the Thouless-Kohmoto-Nightingale-Nijs formula [22] and Fredholm index formula [23–25]. While the latter idea has been generalized to the interacting case, its formalism uses quasiadiabatic evolution and is more convenient to work with if the actual Hamiltonian, rather than a single wave function, is known [26,27]. We also note earlier works on extracting the many-body Chern number from a single wave function based on connections to

topological quantum field theory and surgery [28,29]. This quantity coincides with the Hall conductance in free-fermion systems but is a distinct quantity in generic interacting systems (see Ref. [29] for details).

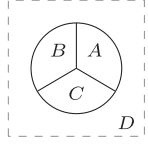
In this Letter, we conjecture a new formula, with analytical and numerical support, which uses entanglement to compute the Hall conductance from a single wave function directly. The formula is proposed for generic interacting systems without assuming translational invariance [30].

The Hall conductance relies on charge conservation, which the entanglement spectrum of a state is blind to [31]. Therefore, more data are necessary, motivating our use of the *modular Hamiltonian* and *modular flow* in the formula presented here. In a recent advance, the modular Hamiltonian has appeared in a proposed formula for the chiral central charge [32,33], which can be viewed as entanglement transport under the modular flow [34]. (See also [20,21] for related works.) Here, we are interested in the Hall conductance  $\sigma_{xy}$ , a distinct topological invariant, which requires an additional conserved U(1) charge  $Q$ .

*Proposed formula for Hall conductance.*—Consider a lattice system on the plane with a U(1) symmetry that is generated by the total charge operator  $Q = \sum_i n_i$ , where  $i$  labels the lattice sites. Let  $|\psi\rangle$  be a U(1) symmetric gapped wave function,  $\rho_D = \text{Tr}_{\bar{D}}|\psi\rangle\langle\psi|$  the reduced density matrix of any given region  $D$ . The modular Hamiltonian is defined as  $K_D := -\ln \rho_D$ , which is a Hermitian operator with a lower-bounded spectrum and conserves the total number of charges  $Q_D$  in that region, i.e.,  $[Q_D, K_D] = 0$ . The modular Hamiltonian generates a unitary evolution  $U_D(s) := e^{-isK_D}$ , called modular flow, where the modular time  $s$  is dimensionless [35]. The Hall conductance is encoded in a charge response under modular flow at the linear order in  $s$ .

Specifically, divide the plane into four regions  $A$ ,  $B$ ,  $C$ , and  $D$ , whose linear sizes are larger than the correlation length, and every three regions meet at a point once and

only once [25,32]. Let  $K$ , and  $Q$ , denote the modular Hamiltonian and charge of the corresponding region. The response function we focus on is



$$\Sigma(\psi; A, B, C) = \frac{i}{2} \langle \psi | [K_{AB}, Q_{BC}^2] | \psi \rangle, \quad (1)$$

i.e., the charge response in  $BC$  under the modular flow on  $AB$ . The modular Hamiltonian itself is nonuniversal and ultraviolet divergent, but the expectation value of the commutator will be argued to be topological and insensitive to details of the wave function. Our proposal for Hall conductance  $\sigma_{xy}$  is

$$\Sigma(\psi; A, B, C) = \sigma_{xy}. \quad (2)$$

Note that the left-hand side containing  $Q_{BC}^2$  is consistent with the fact that the unit of Hall conductance is  $e^2/\hbar$ .

The rest of the Letter presents evidence for this formula from various angles. We first show that the formula shares the same general properties as the Hall conductance. We then establish their quantitative connection via the bulk-edge correspondence and conformal field theory (CFT) arguments. Our discussion, which uses the defect operator, provides a unifying viewpoint on the two different formulas for the chiral central charge and Hall conductance. Finally, we provide numerical evidence using both lattice and continuum free-fermion models.

*General properties.*—Any formula for the Hall conductance needs to meet the following minimal requirements. First of all,  $\Sigma(\psi; A, B, C)$  should be real and additive under stacking, i.e., on combining independent systems:

$$\Sigma(\psi_1 \otimes \psi_2; A, B, C) = \Sigma(\psi_1; A, B, C) + \Sigma(\psi_2; A, B, C), \quad (3)$$

which are clear from its definition. Although additivity may seem trivial, other topological quantities, e.g., the many-body Chern number, do not possess this property [29]. We now show that  $\Sigma(\psi; A, B, C)$  also satisfies other requirements that are not manifest in the construction. It has the same *CRT* transformation rules as the Hall conductance, namely, it (i) is even under charge conjugation:

$$\mathcal{C}: \Sigma(\psi; A, B, C) = \Sigma(\mathcal{C}\psi; A, B, C), \quad (4)$$

and (ii) is odd under the reflection [36]

$$\mathcal{R}: \Sigma(\psi; A, B, C) = -\Sigma(\psi; B, A, C), \quad (5)$$

and (iii) is also odd under the time reversal

$$\mathcal{T}: \Sigma(\psi; A, B, C) = -\Sigma(\mathcal{T}\psi; A, B, C). \quad (6)$$

Furthermore, (iv) it is topological, in the sense that

$$\Sigma(\psi; A, B, C) = \Sigma(\psi; A', B', C'), \quad (7)$$

where  $A', B', C'$  are smoothly deformed subregions with the same topology as  $A, B, C$ . Finally, (v) it is universal

$$\Sigma(\psi; A, B, C) = \Sigma(\psi'; A, B, C), \quad (8)$$

where  $\psi'$  is equal to  $\psi$  deformed by a  $U(1)$  symmetric local operator.

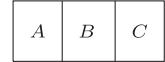
The justification of these properties uses three ingredients. The first one is a conversion formula that follows the Schmidt decomposition

$$K_D |\psi\rangle = K_{\bar{D}} |\psi\rangle, \quad (9)$$

where  $K_D$  and  $K_{\bar{D}}$  are the modular Hamiltonians of the state  $|\psi\rangle$  for an arbitrary region  $D$  and the complement  $\bar{D}$ , respectively. The second is the clustering property, the correlation function of two operators  $O_x$  and  $O_y$  factorizes when their distance  $|x - y|$  is larger than the correlation length  $\xi$

$$\langle O_x O_y \rangle_\psi = \langle O_x \rangle_\psi \langle O_y \rangle_\psi + \mathcal{O}(e^{-|x-y|/\xi}),$$

where  $\langle \cdot \rangle_\psi$  is the expectation value in the state  $|\psi\rangle$ . The third one is an assumption on the decomposition of modular Hamiltonians when they act on the state:



$$(K_{AB} + K_{BC}) |\psi\rangle \approx (K_{ABC} + K_B) |\psi\rangle,$$

where  $A$  and  $C$  do not meet directly [39]. We expect the decomposition to hold when the linear sizes of the subregions are larger than the correlation length. The proof of the *CRT* transformation rules only uses Eq. (9). The argument of the topological rigidity and universal nature uses the other two ingredients as well. The third assumption was also used in [32] to argue the rigidity of the modular commutator formula for the chiral central charge as well.

*Charge conjugation:* The charge conjugation sends the charge operator from  $Q_D$  to  $N_D - Q_D$ , where  $N_D$  is the maximal number charge of the region  $D$ . Here, we have assumed a finite Hilbert space per site. Thus, the right-hand side of Eq. (4) is essentially

$$\langle [K_{AB}, (N_{BC} - Q_{BC})^2] \rangle_\psi = \langle [K_{AB}, -2N_{BC}Q_{BC} + Q_{BC}^2] \rangle_\psi,$$

which can be shown to equal to the left-hand side by using  $\langle [K_{AB}, Q_{BC}] \rangle_\psi = 0$  [36].

*Reflection:* For a symmetric choice of  $A, B$ , and  $C$ , reflection effectively interchanges  $A$  and  $B$ . In fact, Eq. (5)

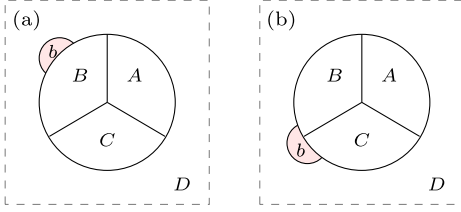


FIG. 1. Geometric deformation. Undeformed regions  $A, B, C$  with: (a) Deformation “ $b$ ” is away from the triple contact points. (b) Deformation is close to one triple contact point.

holds more generally even when  $A, B, C$  have unequal sizes and different shapes. Nevertheless, we still call Eq. (5) the reflection transformation. Proving it is equivalent to showing the vanishing of the following quantity

$$\langle [K_{AB}, Q_{BC}^2 + Q_{AC}^2] \rangle_\psi = \langle [K_{AB}, Q_{BC}^2 + Q_{AC}^2 - Q_{ABC}^2] \rangle_\psi,$$

where we have used  $\langle [K_{AB}, Q_{ABC}^2] \rangle_\psi = 0$  in the second step, i.e., modular flow in  $AB$  does not change the charge in  $ABC$ . Expanding the charge operators in terms of  $Q_A, Q_B$ , and  $Q_C$  gives  $\langle [K_{AB}, Q_C^2 - 2Q_A Q_B] \rangle_\psi$ , which vanishes by using Eq. (9).

**Time reversal:** The time reversal keeps the charge operator invariant. Equation (6) follows from  $\langle \mathcal{T}\psi | \mathcal{T}\phi \rangle = \langle \phi | \psi \rangle$  and the Hermiticity of  $K_{AB}$  and  $Q_{BC}$ .

**Topological:** There are two types of deformation that should be considered: deformations of the boundary between regions that are (1) far from any triple contact point or (2) close to one of them. Typical examples are shown in Figs. 1(a) and 1(b), respectively, where a small blob  $b$  is removed from  $D$  and attached to  $B$ . One can check that  $\Sigma(\psi; A, B, C)$  does not change under either of these two deformations when the size of  $b$  is larger than the correlation length [36].

**Universal:** We deform the state  $|\psi\rangle$  to  $|\psi'_x\rangle \propto |\psi\rangle + O_x|\psi\rangle$  by a  $U(1)$  symmetric local operator at position  $x$ , and show Eq. (8). If  $O_x$  is inside a region and far from any boundary, it follows from the clustering property, which implies that the reduced density matrices and thus modular Hamiltonians of other regions do not change [36]. The case where  $O_x$  is close to a boundary can be justified by exploiting the topological rigidity of  $\Sigma(\psi; A, B, C)$ , similar to the argument in [7].

Although the results thus far are compatible with identifying  $\Sigma \propto \sigma_{xy}$  in Eq. (2), the constant of proportionality must be determined. In particular we need to eliminate the trivial possibility that (2) always vanishes. We turn to this task next.

**Connection to Hall conductance.**—The universal property Eq. (8) allows us to deform the state to a nicer form. Therefore, without loss of generality, we can consider gapped states whose edge can be described by a  $(1+1)D$  conformal field theory (CFT) with the central charge  $c$  and

$\bar{c}$  that quantifies the number of chiral and antichiral edge modes. The modular Hamiltonian of a simply connected region  $D$  with a smooth boundary can be approximated by the same CFT Hamiltonian supported on the boundary  $\partial D$  [7,10]

$$\rho_D = \frac{1}{Z_D} e^{-K_D}, \quad K_D = \beta H_{\text{CFT}}, \quad (10)$$

where  $\beta$  is a nonuniversal constant.  $H_{\text{CFT}}$  is defined by the Virasoro generators  $L_0$  and  $\tilde{L}_0$  that governs the dynamics of the chiral and antichiral modes, respectively

$$H_{\text{CFT}} = \frac{2\pi}{\ell_D} \left( L_0 + \tilde{L}_0 - \frac{c + \bar{c}}{24} \right),$$

where  $\ell_D$  is the circumference of the region  $D$ . Thus,  $K_D$  only generates nontrivial modular flow along  $\partial D$ , where the excitation moves with the speed  $v = \beta$ . In the case with  $U(1)$  symmetry, the CFT is augmented by a holomorphic and antiholomorphic current  $J, \tilde{J}$  at level  $k_L, k_R$ , which characterizes the  $U(1)$  current associated to the chiral and antichiral modes. The Hall conductance is  $\sigma_{xy} = (k_L - k_R)/2\pi$ .

It is more instructive to consider the  $U(1)$  defect operator  $e^{i\mu Q_D}$  and obtain  $Q_D^2$  via Taylor expansion in  $\mu$ . This operator creates a line defect along the boundary of  $D$ , and thus its expectation value  $Z_D(\mu) := \langle \psi | e^{i\mu Q_D} | \psi \rangle$  satisfies an area law

$$\ln Z_D(\mu) = -\alpha \ell_D + \gamma + \dots, \quad (11)$$

where  $\alpha$  is the line tension,  $\gamma$  is universal, and the ellipsis represents terms that vanish in the limit  $\ell_D \rightarrow \infty$  [40]. Our focus is the area law coefficient, which is dictated by the charged Cardy formula [41]

$$\alpha = \frac{(k_L + k_R)\mu^2}{4\pi\beta}. \quad (12)$$

This result is related to the spectral flow of the CFT ground state energy under a  $U(1)$  twist [37]. Its linearity in  $k_L + k_R$  is because the levels physically quantify the number of charged modes. The  $\mu^2$  dependence will play an important role in our following derivation.

We reinterpret the result with a quasiparticle picture. There are chiral and antichiral modes sitting near the boundary  $\partial D$ , the numbers of which are proportional to  $k_L$  and  $k_R$ , respectively. Their correlation across the boundary contributes to the line tension. We can then separate  $\alpha$  into two terms that account for the contribution from the two types of modes

$$\alpha_{\text{chiral}} = \frac{k_L \mu^2}{4\pi\beta}, \quad \alpha_{\text{antichiral}} = \frac{k_R \mu^2}{4\pi\beta}. \quad (13)$$

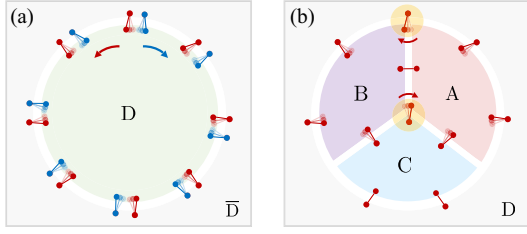


FIG. 2. (a) Red and blue dots are the chiral and antichiral modes, the bonds represent the correlation. The arrows designate their motion under the modular flow  $U_D(s)$ . (b) The antichiral degrees of freedom are suppressed for the clarity of the figure. The arrows designate the motion under the modular flow  $U_{AB}(s)$ . The yellow shaded disks emphasize modes that make contribution to the change of  $Z_{BC}(\mu; s)$  at the linear order in  $s$ .

The idea is sketched in Fig. 2(a), where the chiral and antichiral modes are the red and blue dots, respectively. Under the modular flow generated by  $K_D$ , the chiral and antichiral modes inside the region  $D$  move in opposite directions, as shown by the arrows.

Corresponding to Eq. (1), we apply this picture to compute the response of  $e^{i\mu Q_{BC}}$  under the modular flow generated by  $K_{AB}$

$$Z_{BC}(\mu; s) := \langle \psi | e^{isK_{AB}} e^{i\mu Q_{BC}} e^{-isK_{AB}} | \psi \rangle.$$

It suffices to focus on the chiral modes, the contribution from the antichiral ones is the opposite. See Fig. 2(b). Only the motion of chiral modes that are near the  $ABC$  and  $ABD$  triple-contact points can affect  $Z_{BC}(\mu; s)$  at the linear order in  $s$ . Near the  $ABC$  triple-contact point, chiral modes in  $B$  that are correlated with  $C$  will enter  $A$  and increase the line tension. The  $ABD$  triple-contact point can be analyzed similarly. After summing up the two contributions, we have

$$\frac{d}{ds} \ln Z_{BC}(\mu; s)|_{s=0} = -2(\alpha_{\text{chiral}} - \alpha_{\text{antichiral}})v,$$

where the velocity is  $v = \beta$  as introduced before. By plugging in Eq. (13), we have

$$\frac{d}{ds} \ln Z_{BC}(\mu; s)|_{s=0} = -\frac{k_L - k_R}{2\pi} \mu^2 = -\sigma_{xy} \mu^2. \quad (14)$$

Here, the nonuniversal factor  $\beta$  is completely canceled, which yields a universal answer. This is the main result of this work. Expanding  $e^{i\mu Q_{BC}}$  on the left-hand side above to quadratic order in  $\mu$  gives the right-hand side of Eq. (1) which verifies our identification in Eq. (2). In [36], we apply the same idea to purely 1 + 1D CFTs and show that it detects the perturbative chiral anomaly, which is consistent with the spirit of the bulk-edge correspondence.

*Numerics.*—We provide numerical support to our conjecture by simulating free fermion systems. In this section we report on a lattice model and focus on  $\Sigma(\psi; A, B, C)$  in

different phases, its finite size scaling, and topological rigidity. The noninteger values are attributed to either finite-size effect or the closing of the energy gap. [36] contains other aspects as well as results on a continuum model. In particular, we numerically check the remarkable  $\mu^2$  dependence in the area law coefficient Eq. (12) in lattice systems and find excellent agreement.

We simulate the  $\pi$ -flux model on a square lattice. The Hamiltonian,  $H = \sum_{ij} t_{ij} c_i^\dagger c_j$ , consists of nearest-neighbor hopping terms that implement  $\pi$  flux per plaquette and next-nearest-neighbor hoppings that open a gap and give rise to various phases. We choose a one-dimensional path inside the entire phase diagram that is parametrized by  $\eta \in \mathbb{R}$ . The system is time-reversal symmetric for  $\eta \leq 0$  and breaks the symmetry for  $\eta > 0$ . There is a topological phase at  $0 < \eta < 2$  with a Chern number  $C = 1$  and two trivial phases elsewhere. In the numerics, we also add weak on-site disorders to make the situation more general.

The result of  $\Sigma(\psi; A, B, C)$  across the phase diagram is shown in Fig. 3(a), where we obtain the correct Hall conductance of each phase. Our formula indeed vanishes identically in the time-reversal symmetric region  $\eta < 0$ . Near the two phase boundaries, the curve becomes steeper for larger subsystem sizes. In the topological phase, we perform a more detailed finite size scaling. Let  $\Delta := 1 - 2\pi\Sigma(\psi; A, B, C)$  be the difference between the theoretical and numerical value, and the result is shown in Fig. 3(b). The deviation decays exponentially with the linear size of the subsystem and the decaying exponent is twice of the correlation length. As a sanity check, if  $A, B, C$  form an annulus (replace a disk neighborhood of the  $ABC$  triple-contact point by region  $D$ ) we find a null result. This is consistent with our quasiparticle picture.

We also provide numerical evidence on the topological rigidity as independent support from our analytical argument. For example, we deform the boundaries near the triple-contact points, depicted in Figs. 4(a1)–4(a3), and compute  $\Sigma(\psi)$  for the deformed geometry. As shown in

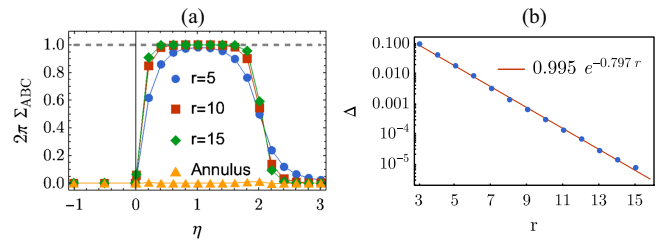


FIG. 3. (a)  $\Sigma(\psi; A, B, C)$  across the phase diagram. Blue, red, and green curves correspond to the disk geometry at the corresponding radii  $r$ . The dashed line is the value of the quantized Hall conductance. (b) Finite size scaling. The blue dots are the data points and the red line is the fitting result. We choose  $L_x = L_y = 40$ . For the annulus geometry, the inner and outer radius is 7 and 14. For (b), the inverse correlation length is  $\xi^{-1} = 0.398$ .

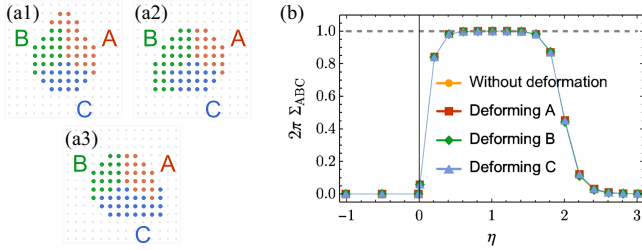


FIG. 4. Topological rigidity against deformation near the triple-contact points. (a1)–(a3) Attach a blob to region A, B and C near the triple-contact point, respectively. (b) Evaluate  $\Sigma(\psi, A, B, C)$  for the deformed geometry across the phase diagram. We choose  $L_x = L_y = 30$  and the radius of the disk  $ABC$  to be  $r = 10$ . The blob has a linear size of 4.

Fig. 4(b), its value remains the same across the entire phase diagram even though the added blobs are not much larger than the correlation length. The results are the same for other deformations.

*Discussion.*—The present results can be understood as linear response extensions that go beyond “static” entanglement features by utilizing the dynamics generated by the modular (or entanglement) Hamiltonian. Here, the charged Cardy formula evaluates the static features of the U(1) twist operator  $e^{i\mu Q}$  [40], and its linear response under the modular flow is shown to give the Hall conductance. We would like to note that the dynamical perspective presented here is distinct from the one discussed in [32] which assumes the equivalence of the modular and physical Hamiltonians. It is important to highlight that our perspective is not only crucial in deriving the main result stated in Eq. (1), but it also points to new potential connections between conventional responses and quantum entanglement. For instance, in free fermion systems with single-charge fermion, we may anticipate an entanglement version of the Wiedemann-Franz (WF) law, which indeed can be obtained by combining the result in [32] and our formula

$$\left\langle \left[ K_{AB}, K_{BC} - \frac{\pi^2}{3} Q_{BC}^2 \right] \right\rangle_{\psi} = 0. \quad (15)$$

Understanding the violation of this entanglement WF law and finding other such relations can shed new light on the study of entanglement of many-body systems.

In addition to connecting entanglement and topological response, our formula also shows how it encodes the boundary ’t Hooft anomaly, which is a natural, albeit less explored, question. Furthermore, it is interesting to generalize our argument to other symmetries and higher dimensions.

Moreover, both the previous work [32] and our formula could aid in understanding the “expressibility” of different variational ansatz wave functions, which is important for numerical simulation of strongly correlated quantum many-body systems. There is a long-standing puzzle whether the

projected entangled pair state (PEPs) is able to represent interacting chiral states [42]. Evaluating these two formulas in PEPs provide a path forward toward solving this question and may shed light on developing new tensor network architecture.

Entanglement entropy suffers from UV divergence in generic Lorentz invariant quantum field theories (QFTs). Distilling universal information from entanglement requires a careful definition of entanglement in QFTs. Our formula, shown to be universal, is an interesting quantity to compute especially in topological quantum field theories. Formulating the calculation in a meaningful way requires a better understanding of multipartite entanglement in QFTs, which is an interesting and nontrivial question in its own right.

We thank John Cardy, Yiming Chen, Meng Cheng, Joel Moore, Huajia Wang, Xi Yin, Carolyn Zhang, and especially Yingfei Gu, Daniel Jafferis, Ari Turner, and Michael Zaletel for many helpful discussions and comments. R. F. and A. V. are supported by a Simons Investigator award (A. V.) and by the Simons Collaboration on Ultra-Quantum Matter, which is a grant from the Simons Foundation (651440, AV). R. F. is supported by the DARPA DRINQS program (Award No. D18AC00033). This work is funded in part by a QuantEmX grant from ICAM and the Gordon and Betty Moore Foundation through Grant No. GBMF9616 to Ruihua Fan. R. S. acknowledges support by the U.S. Department of Energy, Office of Science, Office of Advanced Scientific Computing Research, Department of Energy Computational Science Graduate Fellowship under Award No. DESC0022158.

- 
- [1] X.L. Qi and S.C. Zhang, Topological insulators and superconductors, *Rev. Mod. Phys.* **83**, 1057 (2011).
  - [2] C.-K. Chiu, J.C.Y. Teo, A.P. Schnyder, and S. Ryu, Classification of topological quantum matter with symmetries, *Rev. Mod. Phys.* **88**, 035005 (2016).
  - [3] X.-G. Wen, Colloquium: Zoo of quantum-topological phases of matter, *Rev. Mod. Phys.* **89**, 041004 (2017).
  - [4] B. Zeng, X. Chen, D.-L. Zhou, and X.-G. Wen, Quantum information meets quantum matter—From quantum entanglement to topological phase in many-body systems, *arXiv:1508.02595*.
  - [5] A. Hamma, R. Ionicioiu, and P. Zanardi, Bipartite entanglement and entropic boundary law in lattice spin systems, *Phys. Rev. A* **71**, 022315 (2005).
  - [6] M. Levin and X.-G. Wen, Detecting topological order in a ground state wave function, *Phys. Rev. Lett.* **96**, 110405 (2006).
  - [7] A. Kitaev and J. Preskill, Topological entanglement entropy, *Phys. Rev. Lett.* **96**, 110404 (2006).
  - [8] Y. Zhang, T. Grover, A. Turner, M. Oshikawa, and A. Vishwanath, Quasi-particle statistics and braiding from ground state entanglement, *Phys. Rev. B* **85**, 235151 (2012).

- [9] L. Cincio and G. Vidal, Characterizing topological order by studying the ground states on an infinite cylinder, *Phys. Rev. Lett.* **110**, 067208 (2013).
- [10] H. Li and F. D. M. Haldane, Entanglement spectrum as a generalization of entanglement entropy: Identification of topological order in non-Abelian fractional quantum Hall effect states, *Phys. Rev. Lett.* **101**, 010504 (2008).
- [11] L. Fidkowski, Entanglement spectrum of topological insulators and superconductors, *Phys. Rev. Lett.* **104**, 130502 (2010).
- [12] A. M. Turner, Y. Zhang, and A. Vishwanath, Band topology of insulators via the entanglement spectrum, *Phys. Rev. B* **82**, 241102R (2010).
- [13] F. Pollmann, A. M. Turner, E. Berg, and M. Oshikawa, Entanglement spectrum of a topological phase in one dimension, *Phys. Rev. B* **81**, 064439 (2010).
- [14] B. Swingle and T. Senthil, A geometric proof of the equality between entanglement and edge spectra, *Phys. Rev. B* **86**, 045117 (2012).
- [15] A. Chandran, M. Hermanns, N. Regnault, and B. A. Bernevig, Bulk-edge correspondence in entanglement spectra, *Phys. Rev. B* **84**, 205136 (2011).
- [16] X.-L. Qi, H. Katsura, and A. W. W. Ludwig, General relationship between the entanglement spectrum and the edge state spectrum of topological quantum states, *Phys. Rev. Lett.* **108**, 196402 (2012).
- [17] J. Dubail and N. Read, Tensor network trial states for chiral topological phases in two dimensions and a no-go theorem in any dimension, *Phys. Rev. B* **92**, 205307 (2015).
- [18] T. B. Wahl, H. H. Tu, N. Schuch, and J. I. Cirac, Projected entangled-pair states can describe chiral topological states, *Phys. Rev. Lett.* **111**, 236805 (2013).
- [19] A. Kapustin and L. Fidkowski, Local commuting projector Hamiltonians and the quantum Hall effect, *Commun. Math. Phys.* **373**, 763 (2019).
- [20] K. Siva, Y. Zou, T. Soejima, R. S. K. Mong, and M. P. Zaletel, Universal tripartite entanglement signature of ungappable edge states, *Phys. Rev. B* **106**, L041107 (2022).
- [21] Y. Liu, R. Sohal, J. Kudler-Flam, and S. Ryu, Multipartitioning topological phases by vertex states and quantum entanglement, *Phys. Rev. B* **105**, 115107 (2022).
- [22] D. J. Thouless, M. Kohmoto, M. P. Nightingale, and M. den Nijs, Quantized Hall conductance in a two-dimensional periodic potential, *Phys. Rev. Lett.* **49**, 405 (1982).
- [23] J. Bellissard, A. van Elst, and H. Schulz-Baldes, The noncommutative geometry of the quantum Hall effect, *J. Math. Phys. (N.Y.)* **35**, 5373 (1994).
- [24] J. E. Avron, R. Seiler, and B. Simon, Quantum Hall effect and the relative index for projections, *Phys. Rev. Lett.* **65**, 2185 (1990).
- [25] A. Kitaev, Anyons in an exactly solved model and beyond, *Ann. Phys. (Amsterdam)* **321**, 2 (2006).
- [26] S. Bachmann, A. Bols, W. De Roeck, and M. Fraas, Rational indices for quantum ground state sectors, *J. Math. Phys. (N.Y.)* **62**, 011901 (2021).
- [27] A. Kapustin and N. Sopenko, Hall conductance and the statistics of flux insertions in gapped interacting lattice systems, *J. Math. Phys. (N.Y.)* **61**, 101901 (2020).
- [28] K. Shiozaki, H. Shapourian, K. Gomi, and S. Ryu, Many-body topological invariants for fermionic short-range entangled topological phases protected by antiunitary symmetries, *Phys. Rev. B* **98**, 035151 (2018).
- [29] H. Dehghani, Z.-P. Cian, M. Hafezi, and M. Barkeshli, Extraction of the many-body Chern number from a single wave function, *Phys. Rev. B* **103**, 075102 (2021).
- [30] The close relation between entanglement spectrum (ES) and protected edge states suggests a possible strategy based on the ES. However, typically, translation symmetry needs to be invoked to fully extract information present in the ES.
- [31] One can in principle use the  $U(1)$  resolved ES and study the spectral flow, which, however, requires a continuous family of states and is not convenient to work with.
- [32] I. H. Kim, B. Shi, K. Kato, and V. V. Albert, Chiral central charge from a single bulk wave function, *Phys. Rev. Lett.* **128**, 176402 (2022).
- [33] I. H. Kim, B. Shi, K. Kato, and V. V. Albert, Modular commutator in gapped quantum many-body systems, *Phys. Rev. B* **106**, 075147 (2022).
- [34] R. Fan, From entanglement generated dynamics to the gravitational anomaly and chiral central charge, *Phys. Rev. Lett.* **129**, 260403 (2022).
- [35] R. Haag, *Local Quantum Physics: Fields, Particles, Algebras* (Springer-Verlag, Berlin, 1992).
- [36] See Supplemental Material at <http://link.aps.org/supplemental/10.1103/PhysRevLett.131.186301> for details of the proof, numerics as well as a discussion on related anomaly in conformal field theory, which includes Refs. [37–39].
- [37] A. Schwimmer and N. Seiberg, Comments on the  $N = 2$ ,  $N = 3$ ,  $N = 4$  superconformal algebras in two dimensions, *Phys. Lett. B* **184**, 191 (1987).
- [38] H. Casini, M. Huerta, and R. C. Myers, Towards a derivation of holographic entanglement entropy, *J. High Energy Phys.* **05** (2011) 036.
- [39] A. Kitaev, *Toward a topological classification of manybody quantum states with short-range entanglement, talk at Topological Quantum Computing Workshop* (2011).
- [40] B.-B. Chen, H.-H. Tu, Z. Y. Meng, and M. Cheng, Topological disorder parameter, *Phys. Rev. B* **106**, 094415 (2022).
- [41] P. Kraus, Lectures on black holes and the AdS(3)/CFT(2) correspondence, *Lect. Notes Phys.* **755**, 193 (2008).
- [42] J. I. Cirac, D. Perez-Garcia, N. Schuch, and F. Verstraete, Matrix product states and projected entangled pair states: Concepts, symmetries, theorems, *Rev. Mod. Phys.* **93**, 045003 (2021).